ISSN 0389-4010
UDC 621.452.3.01:
621.541

TECHNICAL REPORT OF NATIONAL AEROSPACE LABORATORY

TR-719T

Analysis of the Effects of Inlet Gas-Flow Conditions on a Highly-Loaded Low-Pressure Axial-Flow Turbine Performance

Atsumasa YAMAMOTO, Hiroyuki NOUSE
Mitsuhiro MINODA, Shigeo INOUE
and Hiroshi USUI

July 1982

NATIONAL AEROSPACE LABORATORY

CHŌFU, TOKYO, JAPAN

Analysis of the Effects of Inlet Gas-Flow Conditions on a Highly-Loaded Low-Pressure Axial-Flow Turbine Performance*

Atsumasa YAMAMOTO,** Hiroyuki NOUSE,** Mitsuhiro MINODA,**
Shigeo INOUE** and Hiroshi USUI**

ABSTRACT

An inlet distortion (ID) test was conducted to determine the effects of inlet pressure and/or inlet flow velocity distortions on overall performance of a highly-loaded axial-flow turbine. Two types of steel wire screens were used to produce two different axisymmetrical inlet distortion patterns. Decreases by a few percent in turbine efficiency due to these distortions were found, especially during the part-loaded operations. Simple analysis methods for the prediction of the effects were also tried.

概　　要

本報の目的は軸流タービンの全体性能に及ぼす入口ガス状態の非一様性（インレットディストーション）の影響を実験的に調べ，かつその影響を理論的に予測する方法を開発することである。そのために，軸流タービン空力試験機の入口案内翼 (IGV) の上流に，非一様な流れを発生するための金網を設けて全体性能及び内部流動の試験を行なった。入口全圧に約3～4％のインレットディストーションのある今回の試験では，タービン膨脹比の小さい部分負荷においては，概ね2～3％の比較的大きな効率低下がみられたが，設計点近傍では1％以下とわずかであった。また，こうした影響を理論的に予測する方法を開発するために，流線法による性能予測計算及び非一様な流れがミキシングする際に生ずる全圧損失を考慮した性能予測計算を行なって今回の実験と比較した結果，後者の計算方法がよく実験の傾向を予測できることがわかった。

NOMENCLATURE

A	Area
a, b, c	Defined in Section 3
C_p	Specific heat
G	Turbine weight flow rate
g	Gravity acceleration
ΔH	Turbine specific heat output per unit flow
J	Work equivalent of heat outlet per unit flow
M	Mach number
N	Turbine revolution speed
P	Total pressure
p	Static pressure
R	Gas constant
r_i, r_0	Radii of inner casing and outer casing
T	Temperature
V	Velocity

(Greek letters)

β	Relative flow angle
γ	Pitch angle

* Received 24 May 1982
**Aeroengine Division

δ	Ratio of IGV inlet (mass averaged) total pressure to standard atmospheric pressure
η	Efficiency
θ	Ratio of IGV inlet total temperature to standard atmospheric temperature
κ	Specific heat ratio
π	Turbine expansion ratio
τ	Turbine torque

(Subscripts)

ID	States under inlet flow distortion
i	*i*-th of radial measuring points
m	After gas mixing
max	Maximum
min	Minimum
t	Total
r	Relative
1	IGV inlet
2	IGV outlet and stator inlet
3	Stator outlet and rotor inlet
4	Rotor outlet and OGV inlet
*	Ratio of corrected value to the design value
–	Average

1. INTRODUCTION

Most of the turbine designs and its performance tests are generally made under an assumption of uniform inlet gas flow condition. In the engine operation, however, the inlet gas flow is not necessarily uniform. Especially at the inlet of high-pressure turbine stage, namely at the exit of combustor, both of the pressure and temperature distributions are rare to be uniform. Also in the low pressure turbine stage, the inlet flow is often not uniform, or is not of expected flow due to various factors such as the wakes of the upstream blade rows. These non-uniformities are considered to have some effects on the overall turbine performance. In these day when much higher efficient engine is desired, it is important, therefore, to determine the extent of the effects.

The present test is focused to study the followings;

1) To know how much extent the overall turbine efficiency variation due to the inlet distortion is,
2) to know whether or not the expected performance of the present turbine designed with a controlled vortex design procedure in order to reduce secondary loss is attained when inlet distortion exists. It has been considered that the secondary flow be promoted with the radial nonuniformities of flow velocities in combination with the flow turning across blade rows, and
3) to improve the design or prediction methods such as the stream curvature method (SCM). Under distorted inlet flow conditions where strong streamline mixings are to be existed, this method would be probably inaccurate since the methods can not take account of the mixings.

2. DESIGN SPECIFICATION OF TEST TURBINE

The present test turbine was constructed mainly to verify the usefullness of the control vortex design concept adopted to the 4-stage low-pressure (LP) turbine of a turbofan engine. The test turbine was made using only the second stage stator and rotor of the LP turbine with

Table 1. Major Design Specifications (2nd Stage Stator and Rotor only, excluding IGV and OGV)

Revolutions	$N/\sqrt{\theta}$ (rpm)	3,155
Mass Flow	$G\sqrt{\theta}/\delta$ (kg/s)	16.46
Expansion Ratio	$\overline{\pi}_{G,2-4}$	1.36
Specific Output	$\Delta H/\theta$ (kcal/kg)	5.21
Loading Factor	ψ (MEAN)	2.23
Flow Coefficient	ϕ (MEAN)	0.96
Turbine Efficiency	η	0.896

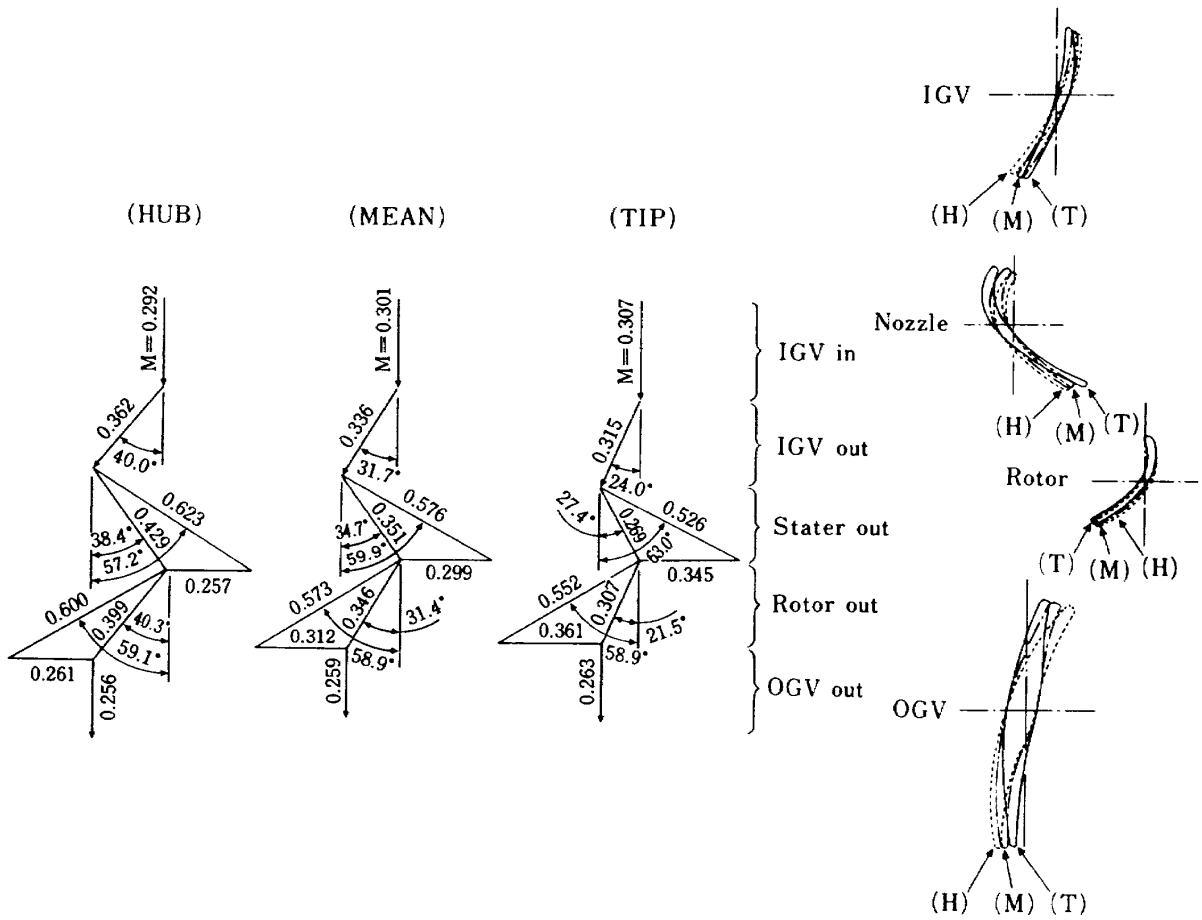

Fig. 1 Design Velocity Triangles

adding inlet guide vanes (IGV) and outlet guide vanes (OGV). The main specifications and the design velocity triangles are shown in Table 1 and in Fig. 1, respectively.

3. PRELIMINARY ANALYTICAL STUDY

Two methods were used to predict the turbine overall performance under prescribed inlet distortions, a streamline curvature method and a mixing loss method.

(a) Streamline Curvature Method (SCM)

With a SCM using the complete radial balance equation by Ngo and Millar [1], a part-load performance calculation were conducted under prescribed inlet total pressure distortions. The calculated results at the design turbine speed are shown in Fig. 2 (a), as well as with the inlet flow conditions. The figure shows that in the case of larger total pressure defect near the outer casing (Case A), the efficiency drops are larger than in Case B at the same turbine expansion ratio and turbine speed. There seems to exist some possibilities of increasing the efficiency in the Case B.

(b) Mixing Loss Method

This method is a simple method taking account of total pressure difference between two conditions of the distorted flow and the corresponding uniform flow, which difference would be caused by gas mixing. The drop of turbine efficiency will be written in the following form.

$$\Delta\eta = \eta_0 \times B \times (1 - e) \qquad (3.1)$$

where η_0 is the efficiency corresponding to design uniform inlet condition, B is a function of turbine expansion ratio and e is a ratio of total pressures;

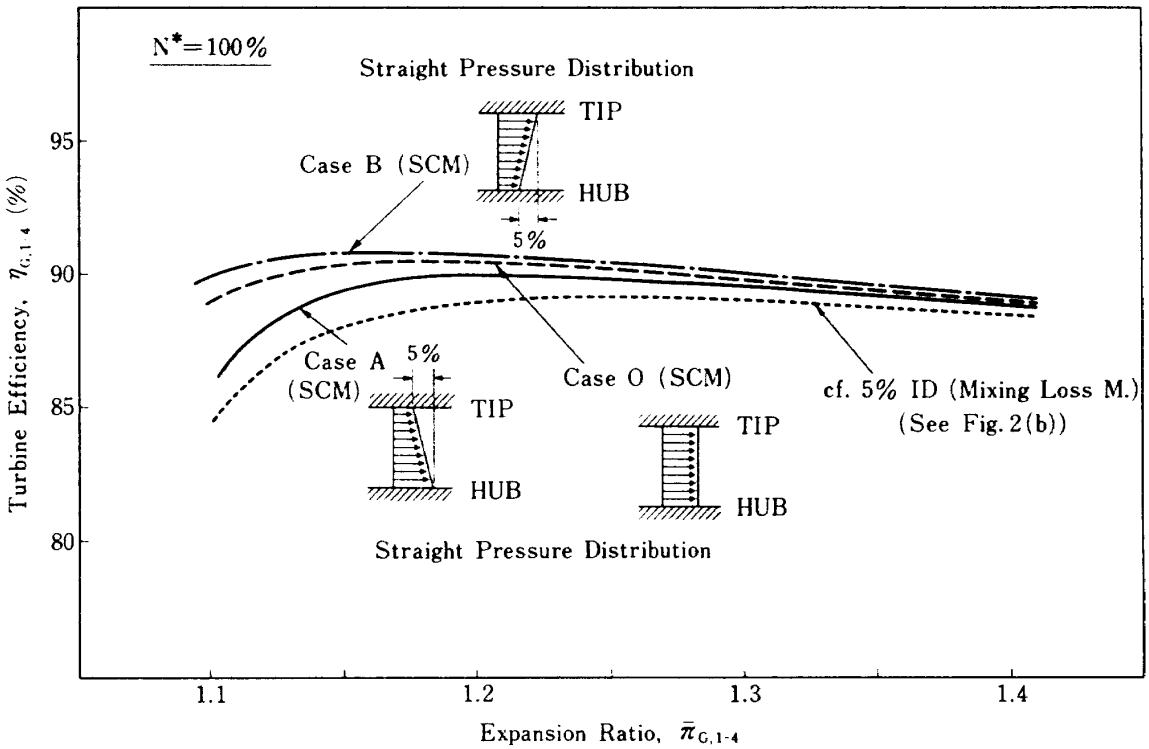

Fig. 2 (a) *ID* Performance Prediction by SCM

$$B = \frac{1-\kappa}{\kappa}\left(\pi^{\frac{\kappa-1}{\kappa}} - 1\right)^{-1} \tag{3.2}$$

$$e = \frac{P_{tm}}{\left(\sum^{i} P_{t,i} G_i \,/\, \sum^{i} G_i\right)_{ID}} \tag{3.3}$$

where, $P_{t,i}$ and G_i denote the local total pressure and local mass flow before the mixing, and P_{tm} is the uniformed total pressure after the mixing obtained from a momentum balance and an equation of continuity;

$$P_{tm} = \sqrt{\frac{R}{kg}}\,\frac{G_m\sqrt{T_{tm}}}{A_m}\,\frac{1}{M_m} \times \left(1 + \frac{\kappa-1}{2} M_m^2\right)^{\frac{\kappa+1}{2(\kappa-1)}} \tag{3.4}$$

$$M_m = \left(\frac{-b-\sqrt{b^2-2a}}{a}\right)^{1/2} \tag{3.5}$$

where,

$$\left.\begin{aligned} a &= \kappa^2\{2-(\kappa-1)c\} \\ b &= 2\kappa - \kappa^2 c^2 \\ c &= \frac{\sum^{i}(A_i p_i g + G_i V_i)_{ID}}{G_m\sqrt{kgRT_{tm}}}\,\frac{A_m}{\sum^{i} A_i} \end{aligned}\right\} \tag{3.6}$$

where, p_i and V_i are the local static pressure and the local velocity before the mixing, respectively.

Results are shown in Fig. 2 (b) with two inlet flow conditions of $ID = 3\%$ and 5%. The result taking only mixing loss into account predicted a littel efficiency reduction of less than 1% near the design point and a few percentage reduction at part-load operations. A merit of this method is to be able to handle arbitrary inlet pressure distortion paterns, while the SCM could not get converged solutions in some arbitrary inlet distortion patterns.

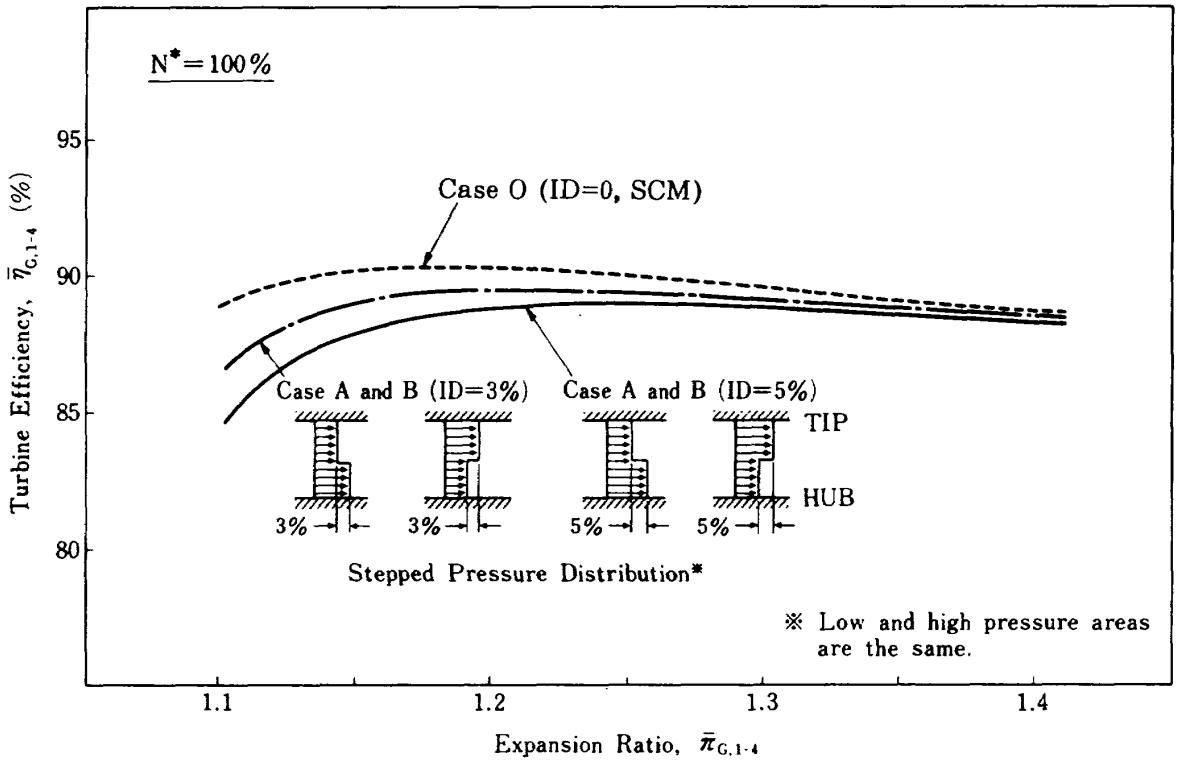

Fig. 2 (b) *ID* Performance Prediction by Mixing Loss Method

4. EXPERIMENTS

4. 1 Inlet Distortion Screens

Two patterns of inlet distortion were produced using two kinds of steel wire screens installed in the turbine test rig (Fig. 3). These screens were consisted of two sheets of large mesh and small mesh JIS standard steel wires, and an inner and an outer rings suporting the wires on the casing walls. The small mesh wire covers over the half area of the large mesh wire as seen in Photo 1. The Case A screen is to produce stronger total pressure defects near the outer casing (near blade tip), while Case B screen near the inner casing (near blade hub).

4. 2 Measurements

The present measurement procedure is the same as described in [2]. Overall performance tests were conducted at three turbine operating points while maintaining constant design speed in the both Cases A and B. At each measuring section of the test turbine shown in Fig. 4, gas conditions were traversely measured in the radial direction with five-head pitot tubes and comb-type thermocouple sensors. Each sensor was fixed at such a circumferencial position that would not include the upstream blade wake region. For comparison of the present *ID* test results with those of uniform inlet flow which we named here Case O, the non *ID* test results, obtained before the present *ID* test, were used. All of the test points adopted in the present report are summerized in Table 2.

4. 3 Data Reduction

The general procedures to obtain the turbine mass flow rate and the turbine torque using JIS standard orifice meter and 970 kw hydraulic dynamometer is the same as described in the previous report [2]. The ways of getting corrected values for the standard atmosphere of

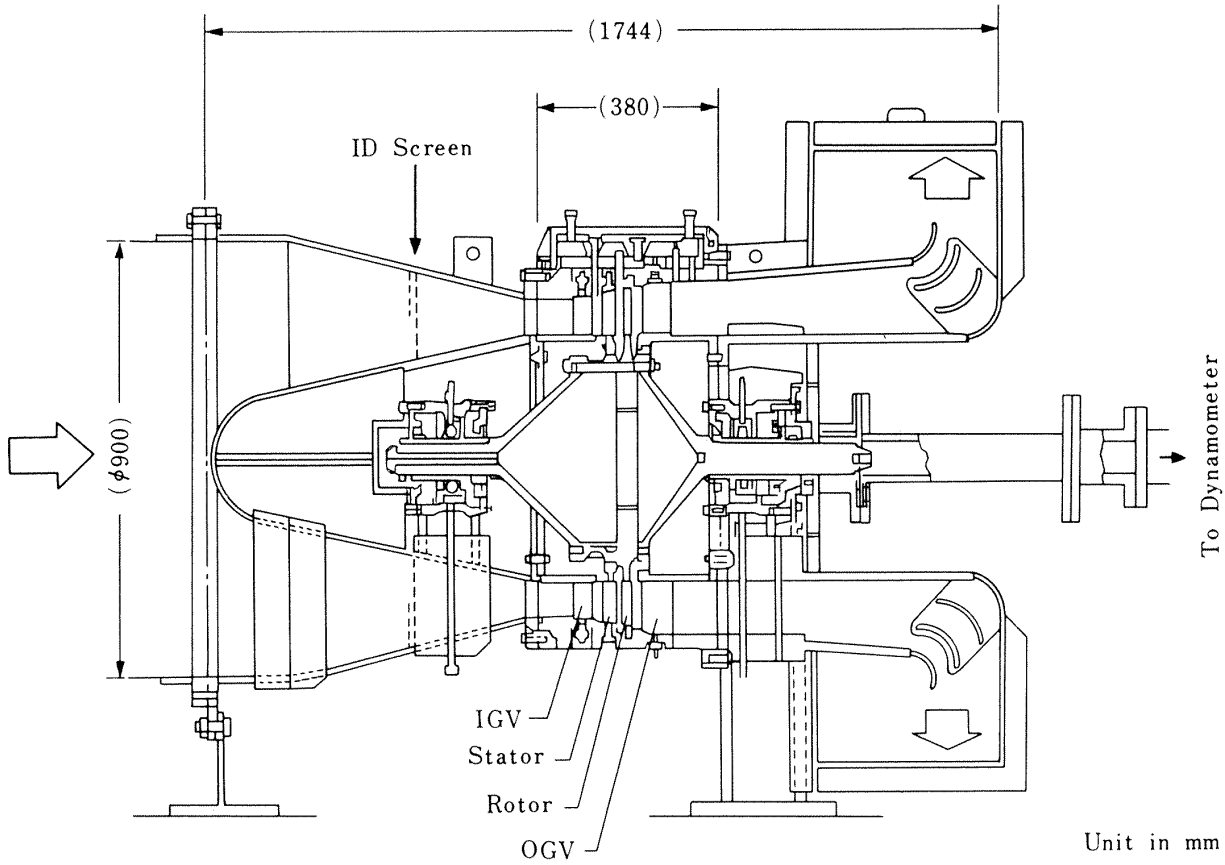

Fig. 3 Sketch of the Highly-Loaded Test Turbine

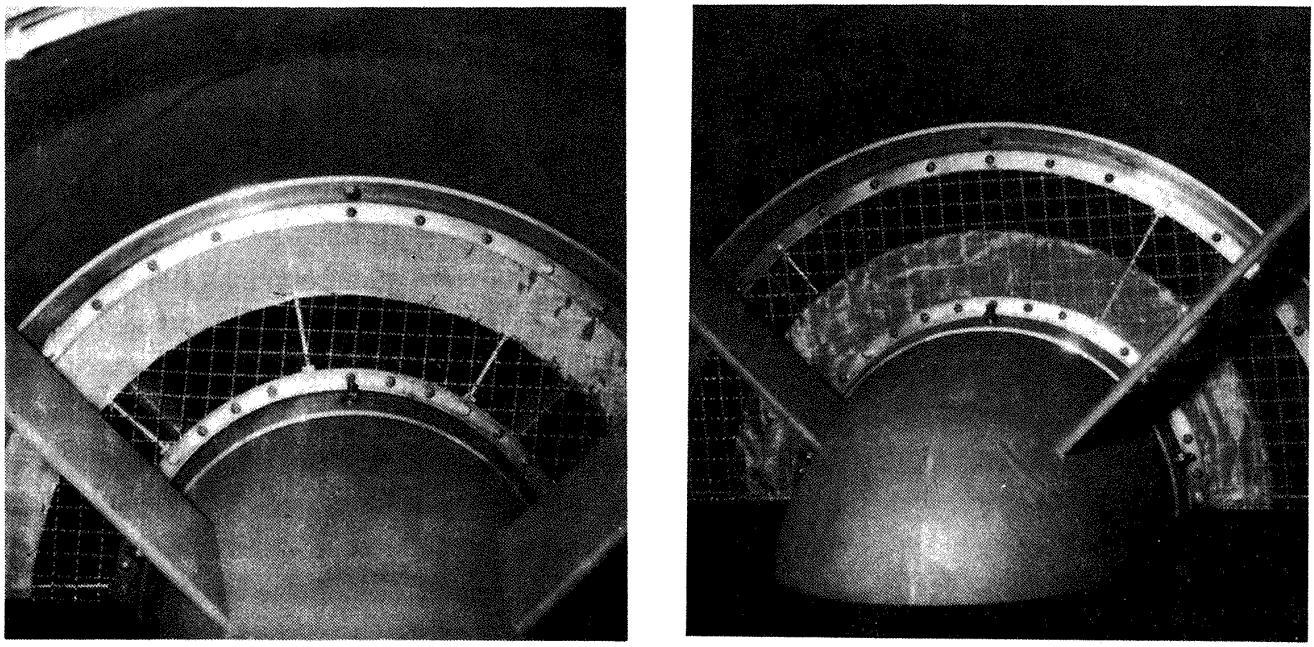

Case A
(Outer Distortion)

Case B
(Inner Distortion)

Photo. 1 Inlet Distortion Screens (Upper half seen from turbine front)

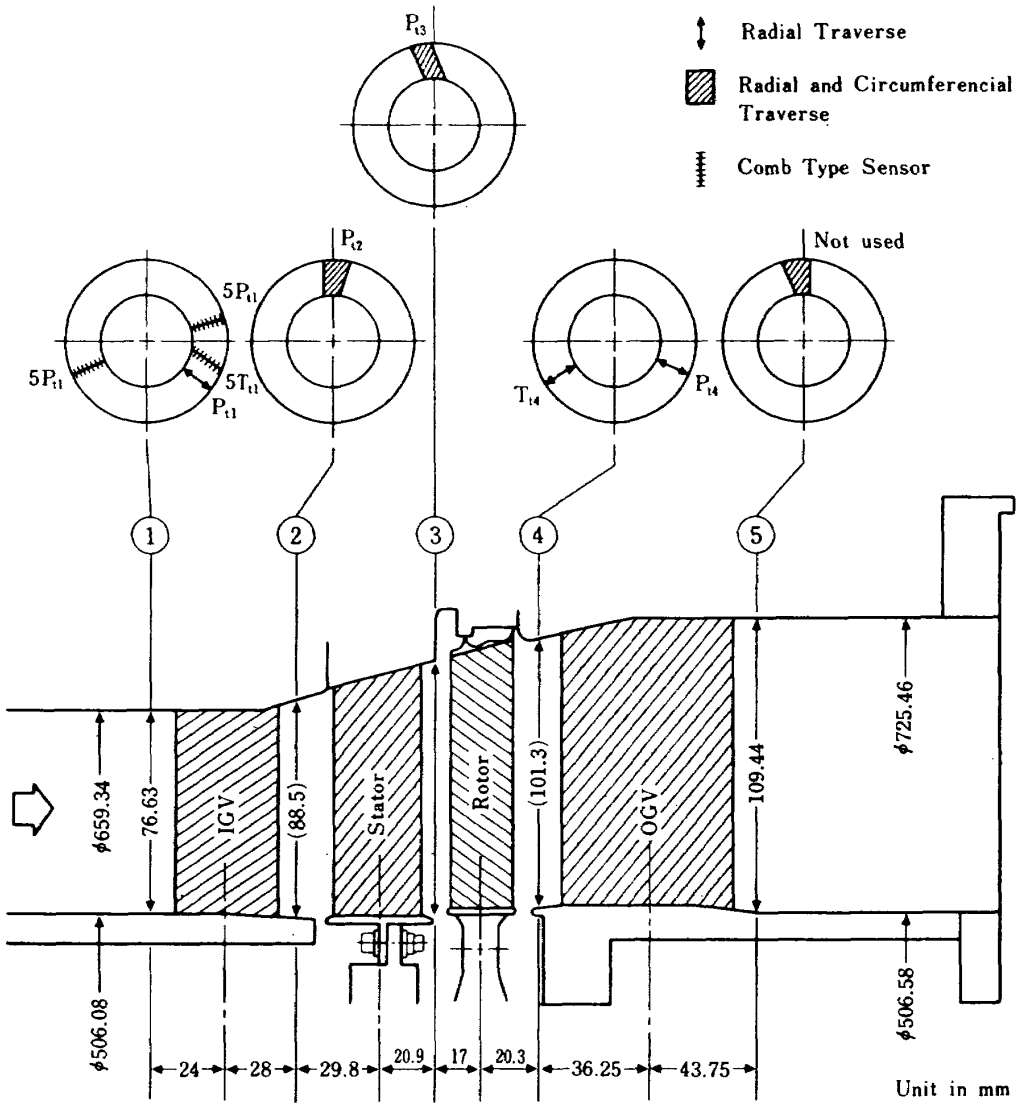

Fig. 4 Measuring Sections and The Cross Section Number

Table 2. Summary of Test Points

Case	$\overline{\pi}_{G,1-4}$	N^* (%)	Measuring Sections	Exp. No.
Case O	1.072	100.0	1, 2, 4, 5	5406191400
	1.191	100.3	2, 3, 4	5411210501
	1.370	99.7	〃	5411210304
	1.375	99.8	1, 2, 4	5406120806
Case A	1.183	101.9	1, 2, 3, 4	5610230201
	1.285	100.0	〃	5610230301
	1.365	99.7	〃	5610230401
Case B	1.184	98.4	1, 2, 3, 4	5610290601
	1.297	100.2	〃	5610290701
	1.356	99.8	〃	5610290801

turbine mass flow rate and specific heat output are the same as those used in [3].

Turbine specific heat output was calculated from turbine torque, revolution speed and mass flow by

$$\Delta H = \pi \cdot \tau \cdot N / (30 J \cdot G) \tag{4.1}$$

Two types of total pressure average were used, i.e., mass average and area average expressing by

$$\overline{P}_{t,G} = \sum^{i} P_{t,i} G_i / \sum^{i} G_i \tag{4.2a}$$

$$\overline{P}_{t,A} = \sum^{i} P_{t,i} A_i / \sum^{i} A_i \tag{4.2b}$$

respectively. The similar two averages were defined for temperatures.

The turbine expansion ratios used for the calculation of turbine efficiencies with (sufix is 1-4) and without (sufix is 2-4) IGV were defined as follows;

$$\bar{\pi}_{G,\substack{1-4\\2-4}\text{ or }} = \bar{P}_{t1\text{ or }2,G}/\bar{P}_{t4,G} \tag{4.3a}$$

$$\bar{\pi}_{A,\substack{1-4\\2-4}\text{ or }} = \bar{P}_{t1\text{ or }2,A}/\bar{P}_{t4,A} \tag{4.3b}$$

Note that the turbine inlet velocity distribution, which were needed to calculate mass averaged values, were obtained by an analysis using the IGV inlet total pressure and total temperature distributions and the turbine mass flow rate experimentally obtained and with an assumption of uniform inlet static pressure (See Appendix Fig. 1). The direct velocity data from the calibrated 5-hole pitot tubes at the inlet were not adopted in the report since the measured Mach number were unreasonably high.

The turbine overall efficiencies of mass average and area average were defined as follows;

Including IGV,

$$\eta_{G\text{ or }A,1-4} = \frac{\Delta H}{C_p \cdot \bar{T}_{t1,G\text{ or }A}\left\{1-\left(\frac{1}{\bar{\pi}_{G\text{ or }A,1-4}}\right)^{\frac{\kappa-1}{\kappa}}\right\}} \tag{4.4a}$$

Excluding IGV for reference only, we calculated the efficiencies as

$$\eta_{G\text{ or }A,2-4} = \frac{\Delta H}{C_p \cdot \bar{T}_{t2,G\text{ or }A}\left\{1-\left(\frac{1}{\bar{\pi}_{G\text{ or }A,2-4}}\right)^{\frac{\kappa-1}{\kappa}}\right\}} \tag{4.4b}$$

The inlet distortion strength was expressed by using the maximum, the minimum, and the mass averaged total pressures at the IGV inlet;

$$ID = \frac{P_{t1,max} - P_{t1,min}}{\bar{P}_{t1,G}} \tag{4.5}$$

5. EXPERIMENTAL RESULTS AND DISCUSSION

5.1 The Inlet Distortion Tested

Fig. 5 shows the inlet total pressure distribution at the IGV inlet. The present *ID* indication ranged from about 3% to 4%. Fig. 6 shows the corresponding inlet velocity distribution,

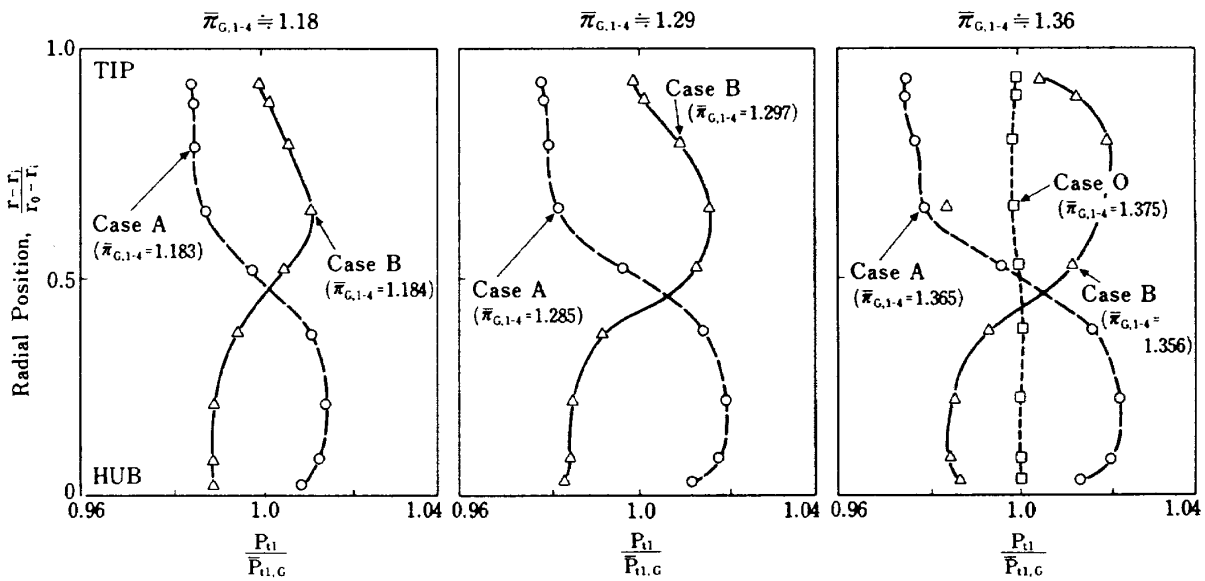

Fig. 5 IGV Inlet Total Pressure Distribution

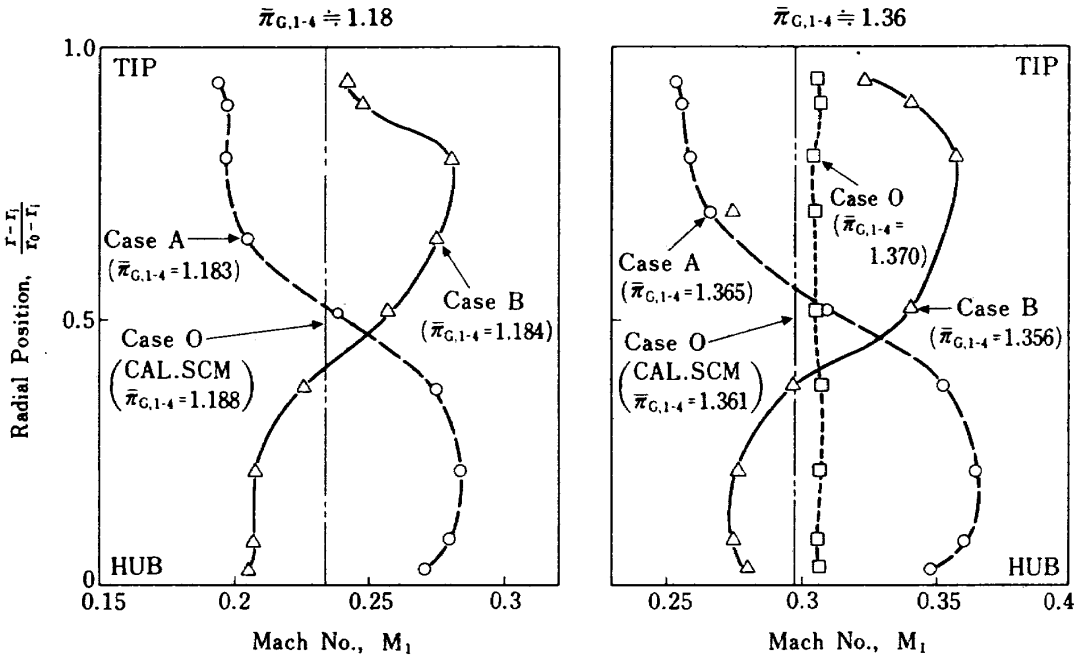

Fig. 6 IGV Inlet Velocity Distibution

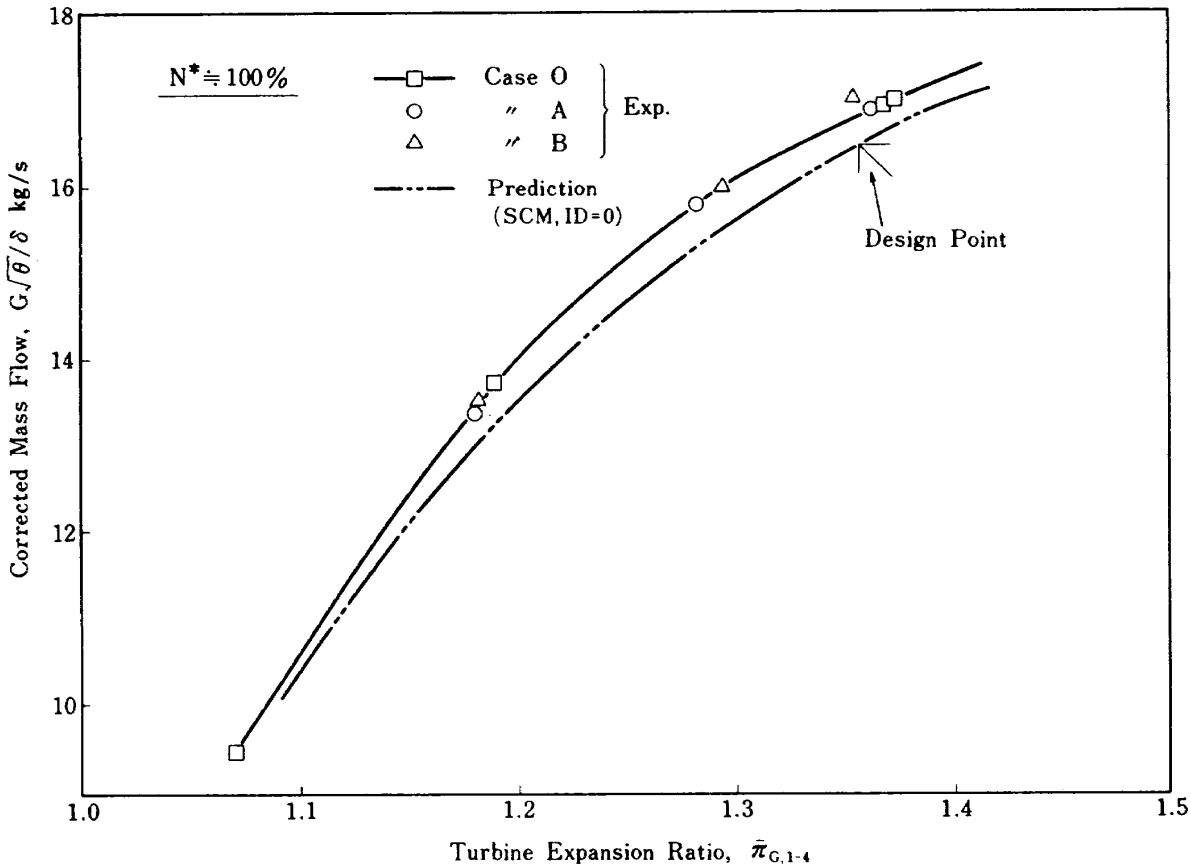

Fig. 7 Mass Flow Characteristic

which means large defect in the mass flow distributions.

5.2 Overall Performance

(a) Turbine Mass Flow and Specific Heat Output

Both the turbine mass flow and the specific heat output characteristics are shown in Figs. 7 and 8 respectively. At the design point, the mass flow was 2.4% larger than the design value, while the specific heat output agreed with the design value correctly. At the part-load operations with nonuniform inlet flow conditions (Case A and B), however, the specific heat output was a little smaller than that with uniform inlet flow (Case O).

(b) Turbine Efficiency

First the mass averaged efficiencies including IGV is discussed. Fig. 9 shows the characteristics of the three cases with and without inlet distortion, in which figure the area average efficiencies are also included only for a reference.

The inlet distortion seems to cause little efficiency reduction at the design point, but has some extent of not negligible reduction in part-load operating regime with small expansion ratio, which was also shown in the previous analysis. Secondarily, for the performance excluding IGV, it should be noted that more detailed measurements at the stator inlet are needed including the circumferential traverse measurements as well as the radial direction surveys. Here in Fig. 10, however, the efficiencies obtained only from the radial survey data is shown. There is seen a difference of the effect between of Case A and of Case B. The corresponding inlet distortions are shown in Figs. 11 (a) and (b).

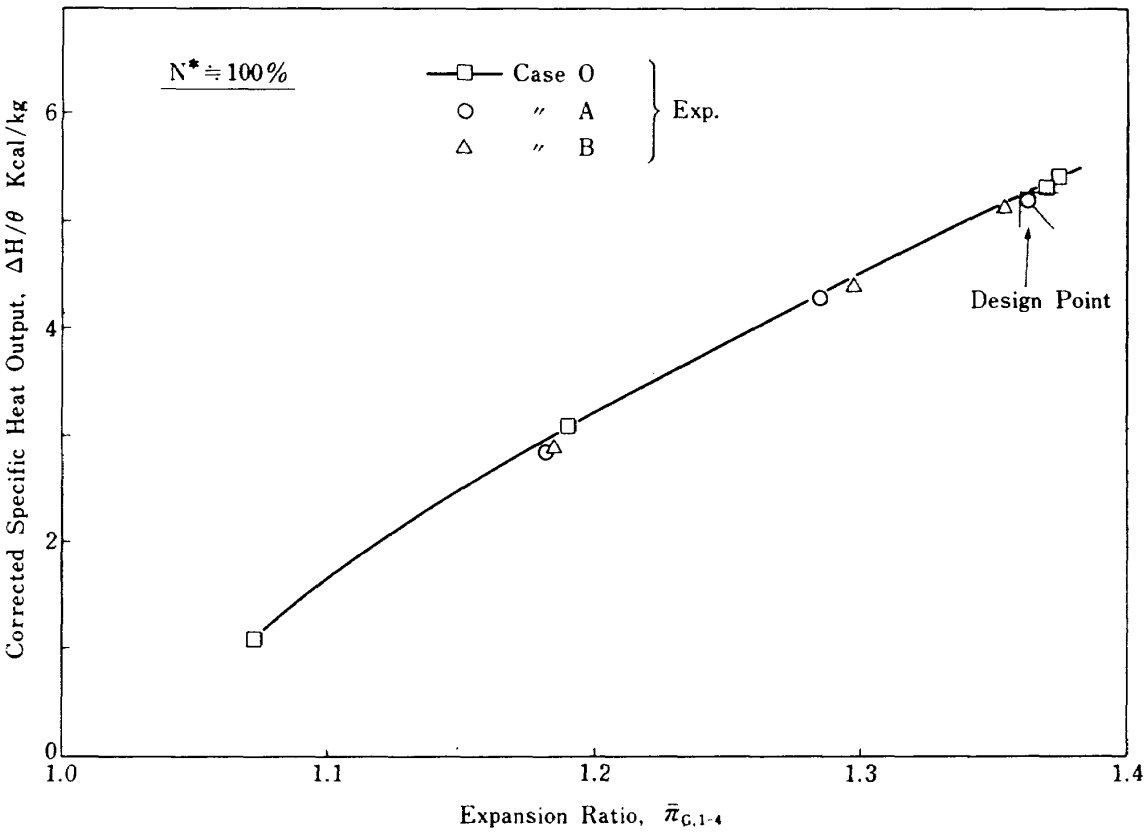

Fig. 8 Specific Heat Output Characteristic

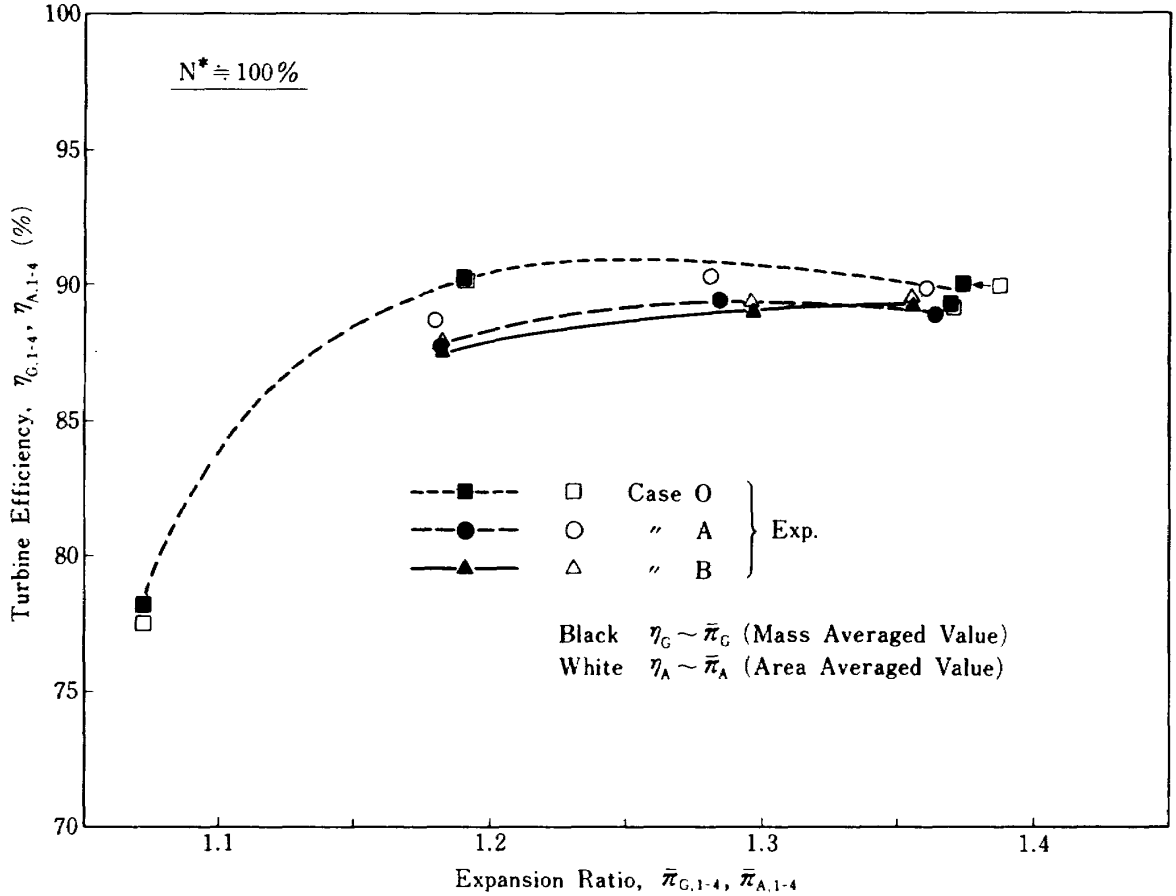

Fig. 9 Turbine Adiabatic Efficiency including IGV

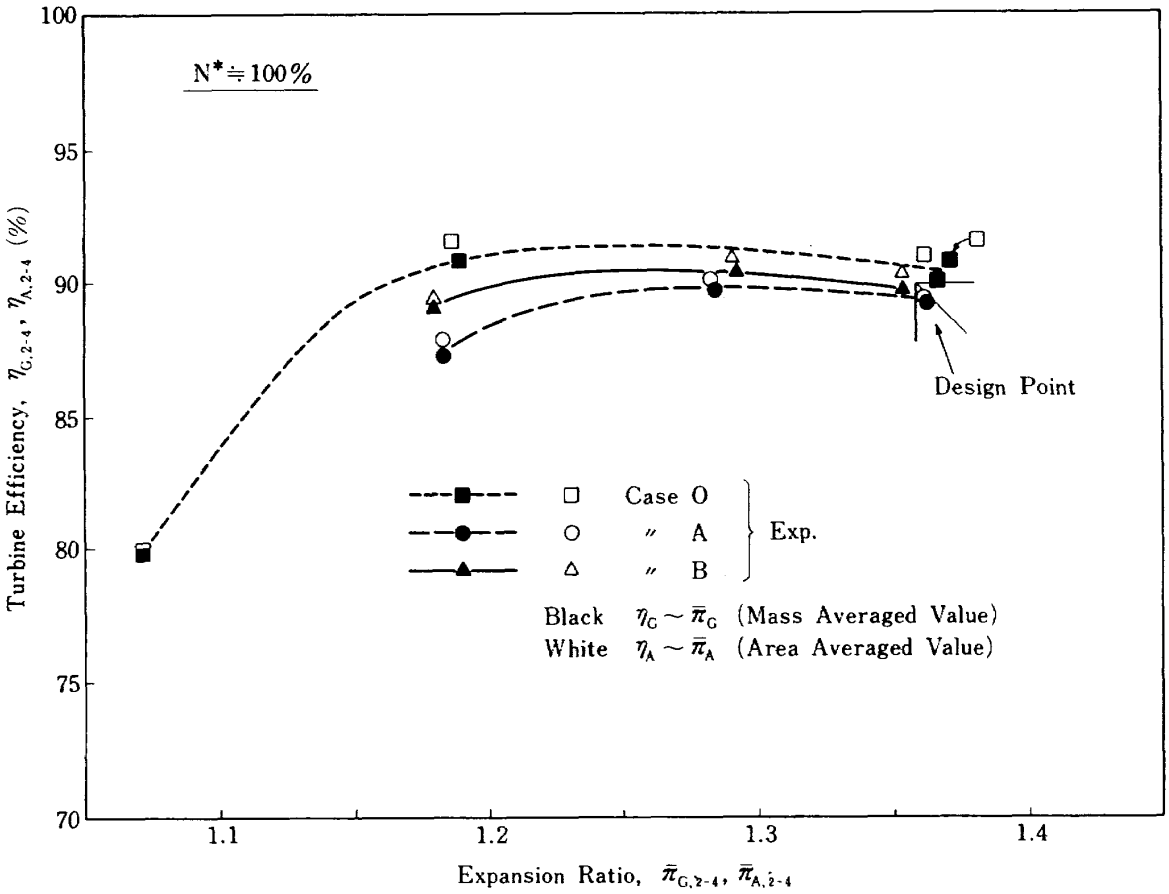

Fig. 10 Turbine Adiabatic Efficiency excluding IGV

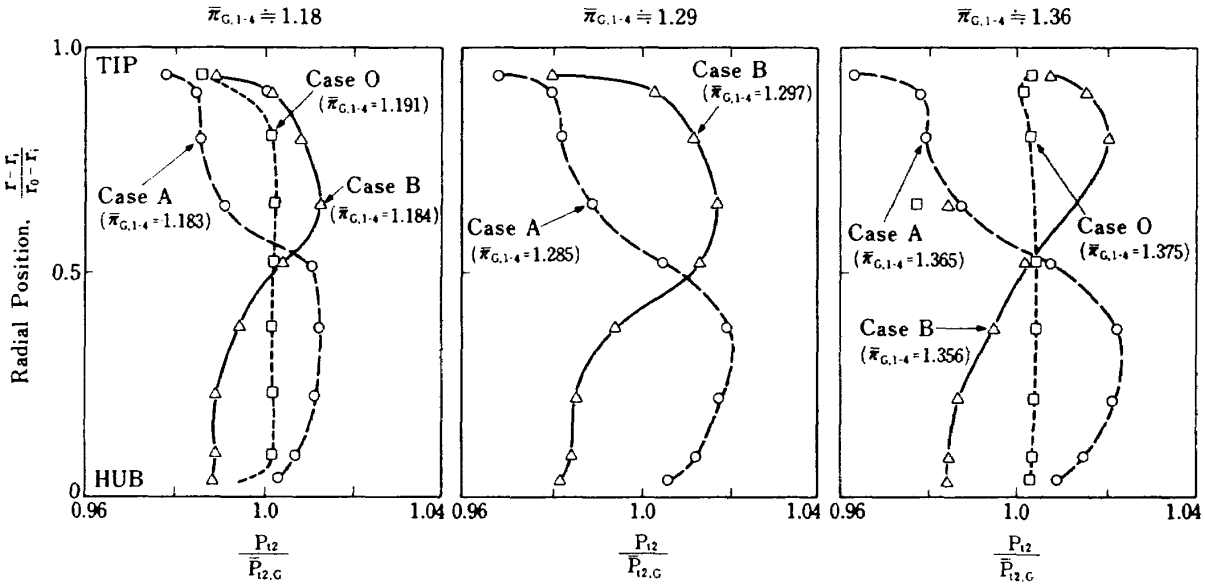

Fig. 11 (a) Stator Inlet Total Pressure Distribution

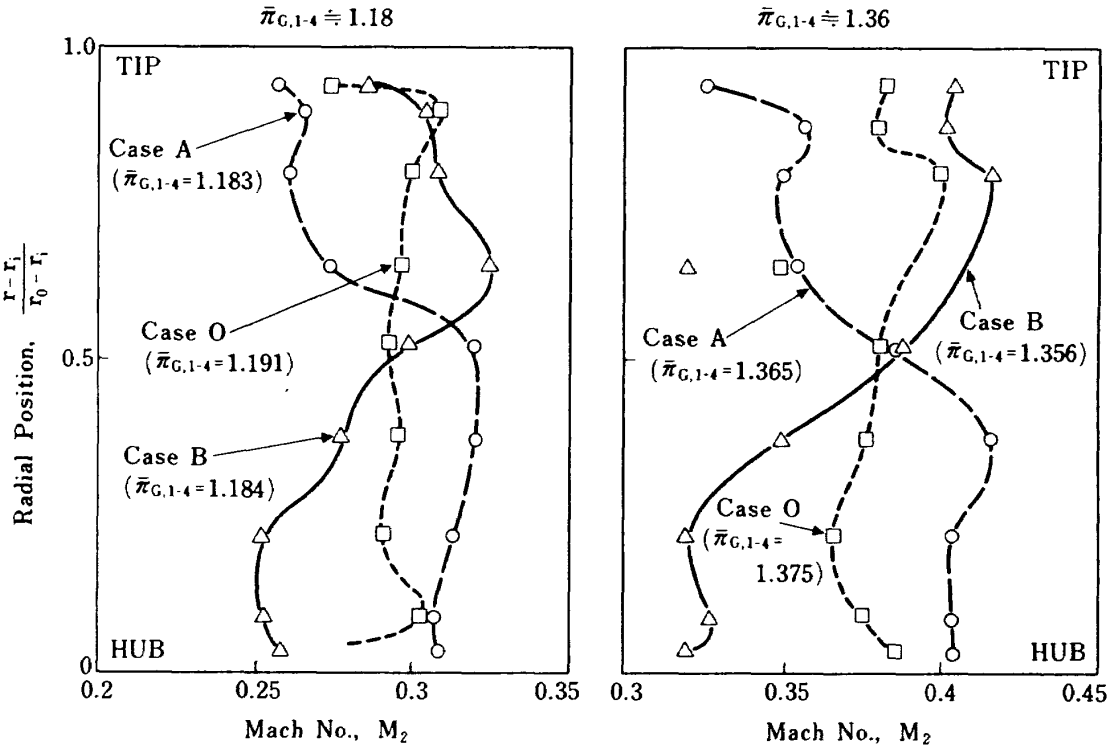

Fig. 11 (b) Stator Inlet Velocity Distribution

Note that in the case of B at $\bar{\pi}_{G,1-4} \fallingdotseq 1.36$, the inlet total pressure distribution shown in Fig. 11 (a) includes wake data. This probably corresponds to a wake of the strut in front of IGV since the same effect was seen in the IGV inlet distortion patterns (Fig. 5). The data were plotted in the figure but not lined.

5.3 Internal Flows

Figs. 12 (a) and (b) show the radial distributions of flows at the inlet and outlet of the rotor at two expantion ratios of about 1.36 and 1.18. One of the major results from the relative inlet and outlet flow angle surveys (β_3 and β_4) at $\bar{\pi}_{G,1-4} \fallingdotseq 1.18$ of Fig. 12 (b) is that the rotor blade turning angles were reduced due to the distortions especially near the both casing walls in the both cases A and B, comparing with Case O. In the Case B, it should be noted that this reduction could not have been predicted by the SCM as seen in Fig. 13. The extent of the experimental reduction of the turning angle was

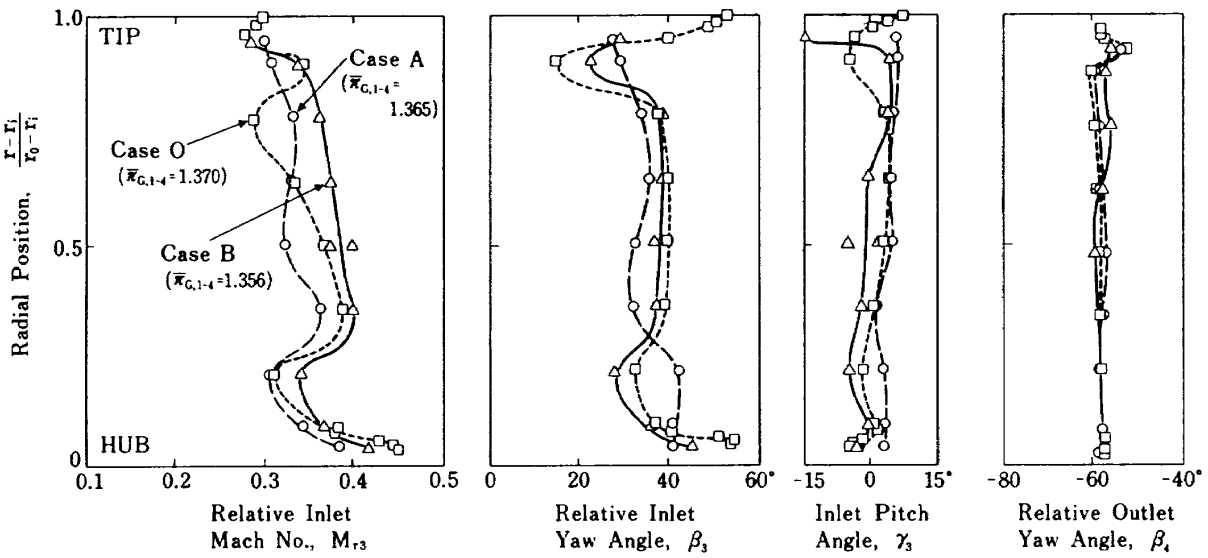

Fig. 12 (a) Effects of *ID* on Rotor Inlet and Outlet Flows (Experimental, $\bar{\pi}_{G,1-4} \fallingdotseq 1.36$)

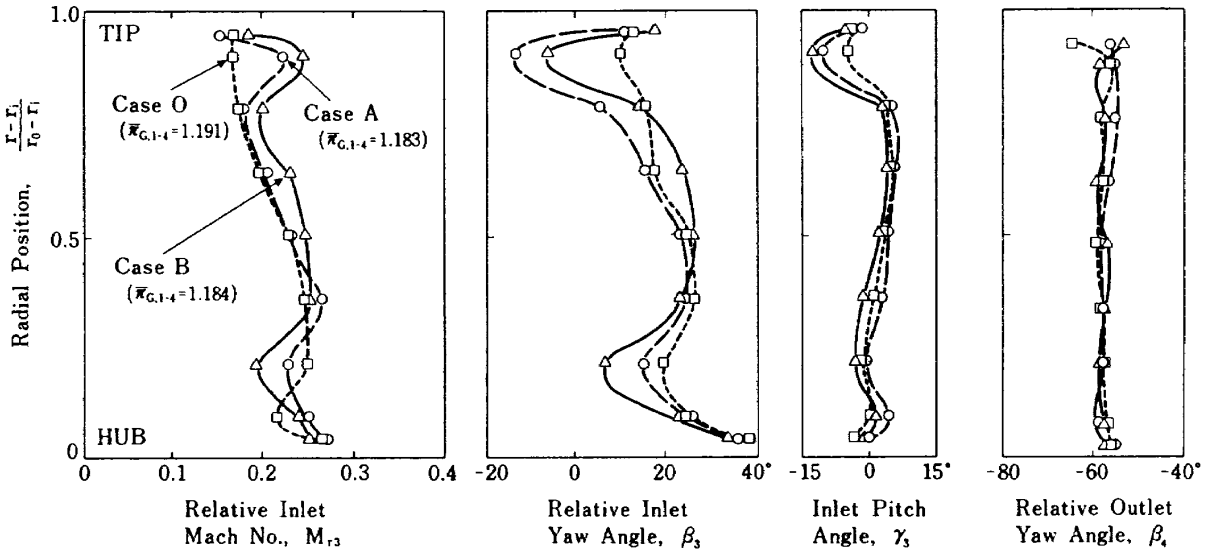

Fig. 12 (b) Effects of *ID* on Rotor Inlet and Outlet Flows (Experimental, $\bar{\pi}_{G,1-4} \fallingdotseq 1.18$)

bigger in Case A than in Case B. The test results indicate that the relative outlet flow angle was little influenced, which was seen also in those of other rows of blades (IGV and Stator). Figs. 12 (a) and (b) include also pitch angles from which streamline defects may be seen. In Fig. 13, several calculated streamline positions are also shown. Since any two neighboring lines include the same mass flow rate, large differences of mass flow distributions could be seen from the figure, which means the change of the blade loading distribution.

6. CONCLUDING REMARKS

An inlet distortion test of a highly-loaded low-pressure axial-flow turbine of a turbofan engine was conducted, using two types of inlet distortion screens in order to change the distributions of inlet total pressure and velocity. The inlet distortions obtained were about 3–4% in the present test.

The major results are as follows;

1) The effect of the inlet distortion on turbine efficiency characteristics is little (less than 1% of efficiency drop) near the design point operation but not negligible (2–3%) at part-load operations with small turbine expansion.
2) The internal flow survey showed that the rotor turning angle near the both casing walls was reduced due to the inlet distortion, which would have resulted in the turbine efficiency drop.
3) Two types of analysis methods (a streamline curvature method and a mixing loss method) were used for prediction of the inlet distortion effects. The latter gave a qualitatively better prediction of the turbine efficiency characteristics. To improve the reliability of the test results applicable to other turbines and to improve the accuracy of prediction methods, further experimental and analytical data should be needed.

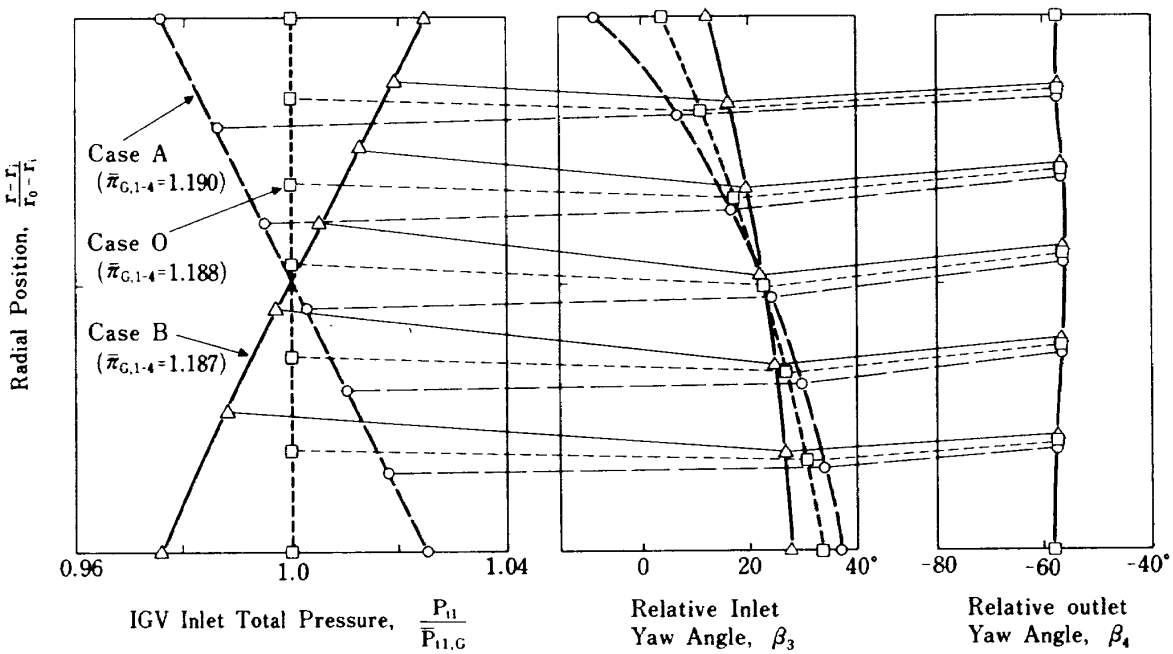

Fig. 13 Effects of *ID* on Rotor Inlet and Outlet Flows
(Predicted by SCM, $\bar{\pi}_{G,1-4} \fallingdotseq 1.19$, $G\sqrt{\theta}/\delta = 13.15$kg/s, $N^* = 100\%$)

7. ACKNOWLEDGEMENT

This study was carried out as a part of the laboratory research of "Research on Reduction of Secondary Flow Losses". The authors would like to express their gratitude to Dr. Masakatsu Matsuki of Deputy Director-General of National Aerospace Laboratory, Mr. Tadao Torisaki of Aeroengine Division Director, Mr. Kitao Takahara of Turbine Section Head, Mr. Hideaki Nishimura of Senior Researcher and Mr. Kenji Nishio of Engine Control Section Head for their helpfull discussion and assistance.

REFERENCES

1. V. H. Ngo and D. A. J. Millar; The Design and Performance Prediction of Axial Flow Turbines, Carleton U. Rept. ME 73-3 (1973).
2. H. Nouse et. al.; An Experimental Study of a High-Loaded and High-Efficiency Axial-Flow Turbine, 21st JSME Aeroengine Meeting (1980).
3. A. Yamamoto et. al.; An Aerodynamic Design and the Overall Stage Performance of an Air-Cooled Axial-Flow Turbine, NAL TR-321T (1981).

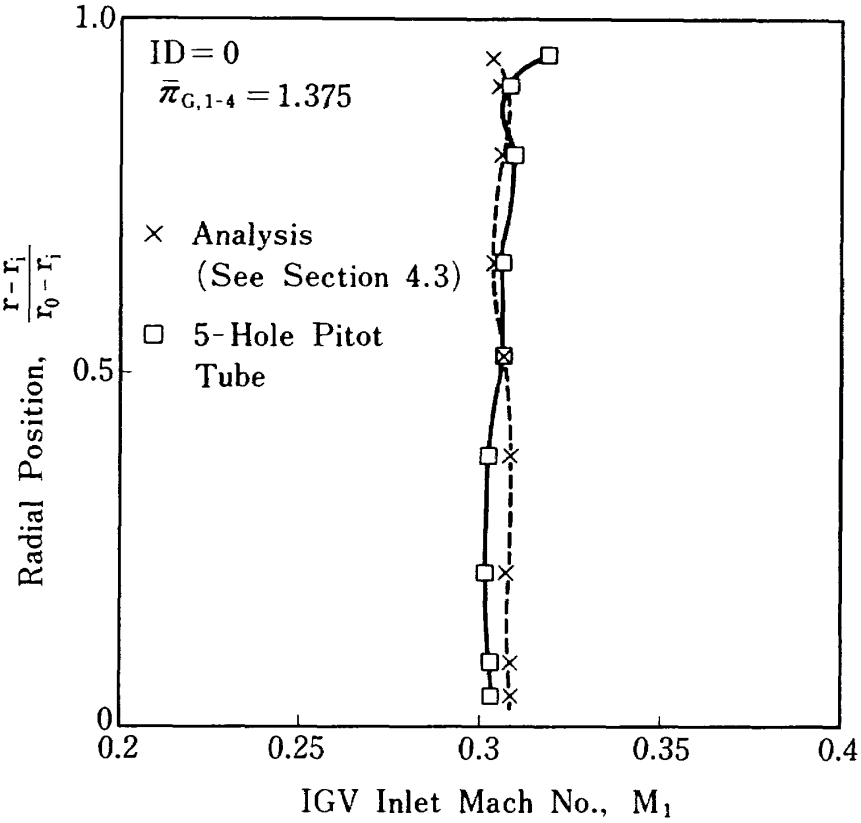

Appendix Fig. 1 Comparison of Analytical and Experimental IGV Inlet Mach No.

TECHNICAL REPORT OF NATIONAL
AEROSPACE LABORATORY
TR-719T

航空宇宙技術研究所報告719T号(欧文)

昭和57年7月発行

発行所 航空宇宙技術研究所
東京都調布市深大寺町1880
電話武蔵野三鷹(0422)47-5911(大代表)〒182
印刷所 株式会社 東京プレス
東京都板橋区桜川2－27－12

Published by
NATIONAL AEROSPACE LABORATORY
1,880 Jindaiji, Chōfu, Tokyo
JAPAN

Printed in Japan